

## **General Disclaimer**

### **One or more of the Following Statements may affect this Document**

- This document has been reproduced from the best copy furnished by the organizational source. It is being released in the interest of making available as much information as possible.
- This document may contain data, which exceeds the sheet parameters. It was furnished in this condition by the organizational source and is the best copy available.
- This document may contain tone-on-tone or color graphs, charts and/or pictures, which have been reproduced in black and white.
- This document is paginated as submitted by the original source.
- Portions of this document are not fully legible due to the historical nature of some of the material. However, it is the best reproduction available from the original submission.

**NASA TECHNICAL  
MEMORANDUM**

**NASA TM X-71776**

**NASA TM X-71776**

(NASA-TM-X-71776) POTENTIAL AND VISCOUS  
FLOW PREDICTION IN V/STOL PROPULSION SYSTEM  
INLETS (NASA) 15 p HC \$3.25 CSCI 21E

**N75-29110**

**Unclas  
G3/07 31437**

**POTENTIAL AND VISCOUS FLOW PREDICTION  
IN V/STOL PROPULSION SYSTEM INLETS**

by Norbert O. Stockman  
Lewis Research Center  
Cleveland, Ohio 44135

TECHNICAL PAPER to be presented at  
Workshop on Prediction Methods for Jet V/STOL  
Propulsion Aerodynamics sponsored by the  
Naval Air Systems Command  
Arlington, Virginia, July 28-31, 1975



POTENTIAL AND VISCOUS FLOW PREDICTION IN  
V/STOL PROPULSION SYSTEM INLETS

by

Norbext O. Stockman

Lewis Research Center  
National Aeronautics and Space Administration  
Cleveland, Ohio

ABSTRACT

Highlights of the method of analysis of inlet flow are given. To indicate the accuracy of the method, several comparisons with experiment for different V/STOL inlet configurations and various operating conditions are given. Two applications to inlet design and analysis are then discussed. A summary of current efforts is given, and finally areas of possible future work are indicated.

E-8434

## INTRODUCTION

Over the past several years a method has evolved at the Lewis Research Center for the calculation of potential and viscous flow in subsonic inlets at arbitrary operating conditions. The development of the potential flow calculations (ref. 1) was originally motivated by the need to design efficient inlets for an in-house lift fan test program (refs. 2 & 3). The method was quite successful at this and was eventually extended to several other VTOL applications (ref. 4).

When the method was applied to STOL inlet designs and analysis, the boundary layer became important, and the boundary layer (or viscous) calculation (ref. 5) was incorporated into the procedure. A status report on the resulting method as of late 1973 is given in reference 6. Since that report many additional applications were made (e.g., refs. 7 & 8).

The present paper will present the highlights of the method itself, several comparisons with experiment, some recent applications of interest, a summary of current efforts and finally a discussion of possible future work.



## SYMBOLS

A, B, C	combination coefficients, eq (1)
a, b	semi-major and minor axis of bisuperellipse, eq (3)
$C_f$	skin friction coefficient (ratio of wall shear stress to dynamic pressure at edge of boundary layer)
D	diameter
M	Mach number
P	pressure
P, Q	bisuperellipse exponents, eq (3)
S	surface distance
V	velocity
$\dot{W}$	inlet mass flow
$\alpha$	inlet incidence angle or angle of attack
$\delta^*$	boundary layer displacement thickness
$\rho$	density

### Subscripts:

c	control station
cor	corrected for compressibility
h	highlight
i	incompressible
j	basic solution, $j = 1, 2, 3$
ref	reference value
t	total or stagnation conditions
th	throat
$\infty$	freestream value

### Superscripts:

 average value  
 vector quantity

## METHOD OF ANALYSIS

The method of analysis is well documented in the literature (refs. 1, 4, 5, 9 & 10), and only the highlights will be presented here. The method comprises the following several steps (shown schematically in fig. 1):

1. Geometry representation (SCIRCL in fig. 1)
2. Incompressible potential flow basic solutions (EOD)
3. Combined solutions with compressibility correction (COMBYN)
4. Boundary layer calculations (VISCUS)
5. Iterative loop

The four computer programs are available from COSMIC, Computer Center, Information Services, 112 Barrow Hall, University of Georgia, Athens, Georgia, 30602. Programs SCIRCL, EOD and COMBYN are one unit with number LEW-12152; program VISCUS is number LEW-12178.

### Geometry

The inlet is assumed to be axisymmetric and is represented by its meridional profile. This profile is broken into segments at convenient tangent points as shown in figure 2. Each segment may be defined by an analytic expression or a set of points. The inlet duct walls and the outer surface (nacelle or bellmouth) must be extended far downstream (fig. 2) to facilitate obtaining accurate potential flow solutions in the inlet region of interest. The geometry program (SCIRCL, fig. 1) prepares coordinate-point input for the potential flow program and also prints out information such as curvature, wall angles, area distribution, etc., which is useful in preliminary screening of proposed inlet shapes.

### Incompressible Potential Flow

The Douglas axisymmetric incompressible potential flow computer program (EOD, ref. 9) is then used to obtain three independent basic solutions. These three basic solutions  $\bar{V}_j$ ,  $j = 1, 2, 3$  are then combined (program COMBYN, fig. 1) into a solution of interest having arbitrary flow conditions of  $V_\infty$ ,  $\alpha$ , and mass flow  $\dot{W}$  (fig. 3). The combination equation is:

$$\vec{V} = A\vec{V}_1 + B\vec{V}_2 + C\vec{V}_3 \quad (1)$$

where A, B, and C are obtained from the flow conditions. Thus, once the basic flow solutions are obtained for a specified geometry, any solution of interest for that geometry can be obtained without repeating the more time-consuming potential flow calculations.

### Compressibility

The velocity obtained by equation (1) is incompressible and is corrected for compressibility by the Lieblein-Stockman compressibility correction (ref. 11).

$$V_{\text{cor}} = V_1 \left( \rho_t / \bar{\rho} \right)^{1/2} \bar{V}_1 \quad (2)$$

where all the terms on the right hand side are obtained from the incompressible flow solution or the input flow conditions. From the velocity other flow properties (Mach number, pressure ratio, streamlines, etc.) are obtained.

### Viscous Flow

The surface Mach number distributions obtained from program COMBYN are used as input to the Herring-Mellor boundary layer calculation (program VISCUS, fig. 1). Reference 5 contains a complete documentation of program VISCUS and references to the original sources. Program VISCUS calculates boundary layer profiles, displacement thickness  $\delta^*$ , skin friction coefficient  $C_f$ , etc., at each station, and also predicts transition from laminar to turbulent flow and separation (whether laminar or turbulent).

### Iterative Loop

If the boundary layer is significant in the inlet region of interest it may be desirable to add the displacement thickness  $\delta^*$  to the original inlet profile and repeat the entire solution procedure, thus obtaining a new Mach number distribution, new  $\delta^*$ , etc.. This process may be iterated to satisfactory convergence. Usually one iteration is sufficient. In parametric studies or preliminary design screening often no iteration is needed.

### COMPARISON WITH EXPERIMENT

To indicate the accuracy of the various aspects of the prediction method several comparisons with experimental data will be given. These will range over incompressible flow, compressible flow with

insignificant boundary layer and viscous flow with various conditions of the boundary layer.

### Incompressible

The surface pressure distributions in a chordwise cut of a fan-in-wing inlet are shown in figure 4. Three surfaces are shown on the plot; the forward surface of the bellmouth, the centerbody and the aft surface of the bellmouth. The agreement between theory and experiment is quite good everywhere on the inlet. This case is included to illustrate the adequacy of the method of geometry representation even when the calculational model (see fig. 2(b)) differs rather significantly from the real geometry.

### Compressible

The next case illustrates the applicability of the method when the flow is compressible. Figure 5 shows the theoretical and experimental surface pressure distributions on a fan-in-pod inlet (described in ref. 3). Both incompressible and incompressible-corrected-for-compressibility theoretical curves are given. The experimental static pressures agree quite well with the theory corrected for compressibility along the entire surface of the inlet.

### Viscous

A translating-centerbody sonic inlet in the retracted configuration (fig. 6(a)) is used for comparing theoretical boundary layer results with experimental. Various conditions of the boundary layer are obtained by varying the inlet incidence angle  $\alpha$ . In all cases, the one-dimensional throat Mach number is 0.50 and the freestream Mach number is 0.13 (these results are all taken from ref. 8).

Boundary layer attached. - Surface Mach number distributions for zero incidence angle are shown in figure 6(b). Two theoretical curves are shown to illustrate the effect of the boundary layer on the surface Mach number. The solid curve is the potential flow alone (no  $\delta^*$  correction); the broken curve is the potential flow obtained with  $\delta^*$  added to the inlet profile and is in excellent agreement with the theory. No separation is indicated either by theory or by experiment.

Diffuser separation. - Results are shown in figure 6(c) for an incidence angle of  $40^\circ$ . Here the theory, with or without the  $\delta^*$  correction predicts separation at about the same point as the experimental data indicate the start of a "pressure plateau" commonly associated with observed separation.

Lip separation. - On figure 6(d) results are given for an inlet incidence angle of  $50^\circ$ . The theoretical Mach number distribution is what would be obtained if the inlet did not separate. The experimental data clearly indicate separation on the inlet lip. The theory also predicts lip separation and although possibly not at the exact point as experiment, it is probably adequate as a guide in inlet design.

In cases where the theory predicts separation the calculations stop and there is no  $\delta^*$  beyond the point of separation. In such cases the distribution of  $\delta^*$  into the separated region is obtained by extrapolation using an unseparated case (lower  $\alpha$ ) as a guide (see ref. 8).

Additional comparison for this and other configurations can be found in reference 8. On the basis of these results, the theory seems adequate in predicting the boundary layer behavior for this type of inlet configuration.

## RECENT APPLICATIONS

Two recent applications of the theoretical method to inlet design and analysis will be discussed. One involves only potential flow and the other viscous flow.

### Potential Flow

This example is taken from a theoretical screening study of inlets for the Quiet Clean Short-Haul Experimental Engine (QCSEE) Project (ref. 7). This study was undertaken to ensure that a reasonable range of contraction ratios was chosen for experimental evaluation. Figure 7 shows the effect of the internal lip contraction ratio,  $(D_H/D_T)^2$ , on the surface Mach number distribution at QCSEE takeoff conditions ( $M_{th} = 0.79$ ,  $M_\infty = 0.12$ ,  $\alpha = 50^\circ$ ). The figure shows that the higher the contraction ratio, the better the Mach number distribution, i.e., the lower the peak and the less severe the unfavorable gradient. (However, the takeoff performance must be compromised with the cruise performance, and the highest contraction ratio lip may not be best overall.)

### Viscous Flow

The sonic inlet of figure 6(a) will be used to illustrate an application of the viscous flow calculation to inlet design. The distribution of theoretical skin friction coefficient as a function of surface distance from stagnation point to diffuser exit is shown in figure 8 (taken from ref. 8). The flow conditions are  $M_{th} = 0.50$  and  $M_\infty = 0.13$  at several values of incidence angle.



The criterion for separation prediction is that the skin friction go to zero, therefore a local minimum with a low value of  $C_f$  is a point of likely separation as the operating conditions become more severe. The zero incidence curve indicates two regions of possible boundary layer separation (at the two minimums), one in the diffuser (where the flow is turbulent) and the other on the internal lip (where the flow is initially laminar).

At an incidence angle of  $20^\circ$ , separation is indicated in the diffuser. As incidence angle is increased further up to  $40^\circ$  the separation point moves upstream somewhat but remains in the diffuser at a position close to the diffuser wall inflection point ( $S \approx 0.6$ ). At  $50^\circ$  incidence, however, the separation point jumps to the lip.

Experimental results for this inlet indicate that diffuser separation in the region of  $S = 0.6$  leads to only small losses whereas lip separation leads to intolerable losses. Thus, it appears that a distribution of  $C_f$ , like that of figure 8, is undesirable and if possible the inlet design should be modified to raise or eliminate the minimum on the lip.

#### CURRENT WORK

This section will briefly discuss several areas of ongoing work and work planned for the immediate future. These areas fall under two general headings: investigation of the method itself; and applications of the method.

##### Investigation of Method

Potential flow. - Improved methods of solution of the incompressible potential flow were recently obtained on contract from Douglas Aircraft Company (ref. 12). These improvements were incorporated into the calculation procedures and are currently being evaluated both by internal program checks and by comparison with experiment. Preliminary results indicate increased accuracy and reduced computer times.

Viscous flow. - The flow in an axisymmetric inlet at angle of attack is three-dimensional, that is, in general, there is a circumferential component. The boundary layer calculations being two-dimensional neglect this circumferential component. Along the windward meridian there is no potential flow circumferential component and the method should be at its best here. The data presented herein seem to indicate that the method is adequate here. At other circumferential locations, however, the method may be inadequate since the boundary layer calculations proceed along a meridian and neglect the circumferential component of flow and the consequent spiral streamline.

To evaluate the adequacy of the method at various meridians, an investigation is underway in which experimentally-determined boundary-layer profiles obtained at several circumferential positions will be compared with calculated profiles. Hopefully this study will establish conditions under which the method is adequate and make recommendations for changes in the method where it is not adequate.

### Applications

Scale effects. - Most inlet testing, particularly that involving setting separation bounds, is done on relatively small scale models. It is generally not feasible to adequately investigate scale effects experimentally, certainly not up to full scale. However, scale effects can be investigated to a limited degree by the existing program. The effects of Reynolds number and wall curvature are included in the program, and thus geometrically similar inlets at different scale will have different calculated boundary layer development. At present the program does not include the effect of scale on shock-boundary layer interaction or on more complex transition mechanisms (such as laminar separation with turbulent reattachment). An investigation is now underway to study the effects of scale within the present limitations and to recommend improvements in the modeling of the transition process. It is hoped that eventually the boundary layer behavior at any scale may be confidently predicted.

Unsymmetrical inlets. - Some inlets of current interest are not axisymmetric, e.g., the scoop inlet (shown in figure 9) designed for reduced downward directed noise and low foreign object damage. A study is getting underway to investigate means of approximately analyzing the flow in such inlets using the axisymmetric programs. If the skew angle is relatively small an equivalent angle of attack approach will be used, i.e., the inlet will be analyzed as if it were an axisymmetric inlet operating at some equivalent artificial angle of attack related to the actual angle of attack and the inlet skew angle.

Tilt-nacelle lip design. - Some V/STOL propulsion system designs may involve a tilting nacelle. This means the inlets must operate efficiently under the conflicting requirements of vertical flight ( $V_\infty = 0$ ), crossflow (with conditions at transition possibly as severe as  $V_\infty = 120$  knots and  $\alpha = 100^\circ$ ) and at high speed cruise. The feasibility of using a fixed geometry lip on this type of inlet will be studied by theoretically investigating several possible lip shapes.

Bisuperellipse diffuser walls. - Most of the diffuser walls used in experimental and analytical studies at Lewis have been cubics. Once the diffuser length and the fan and throat diameter have been chosen a cubic is determined. However, with a bisuperellipse

$$(x/a)^P + (y/b)^Q = 1.0 \quad (3)$$

only a and b are determined and P and Q are still free. This means that the location of the inflection point and its slope (i.e., the maximum wall angle) can be specified. (When either P or Q is less than 1.0 and the other greater than 1.0 the curve has an inflection.) It is proposed to do a parametric study of the effect of the location of the inflection point and the maximum wall angle with the hope of obtaining shorter and more efficient diffusers than those in current use.

#### FUTURE POSSIBILITIES

A few areas of possible future study will be briefly mentioned. These studies would be made only if a real need is indicated and if sufficient time and manpower are available.

##### Modification of Potential Flow Calculations

It seems feasible to modify the calculations in the COMBYN program to account in an approximate way for local total pressure losses along the walls and possibly also the effect of shocks.

##### Modification of Boundary Layer Calculations

As was stated previously the boundary layer calculation proceeds along a meridian and neglects any circumferential velocity component. However, this circumferential velocity component is available in the potential flow results and could be used to construct a spiraling three-dimensional streamline along the inlet surface. The velocity distribution along this streamline could be input to the boundary layer program. There the boundary layer calculation could proceed along a more realistic streamline and the results should better approximate the real flow, at least to the degree that the current method approximates the flow along the windward meridian.

Another shortcoming of the boundary layer calculation is the neglect of shock interactions. Since many cases of current interest contain regions of local supersonic flow it may be necessary to account for possible shock-boundary-layer interaction in the boundary layer calculations.

Finally, the program is not able to predict separation bubbles that appear to be present in the experimental data. However it might be feasible to include the predictions of a separation bubble in an improved transition model.

### Three-Dimensional Analysis

It seems likely that eventually a more accurate analysis of unsymmetrical inlets will be required than that obtainable from the axisymmetric programs. In this eventuality, the Douglas three-dimensional potential flow program could be modified to handle the desired arbitrary input flow conditions ( $V_\infty$ ,  $\alpha$ ,  $\dot{W}$ ) and to include compressibility and boundary layer calculations comparable to those now included in the axisymmetric calculations.

### CONCLUDING REMARKS

A method for the prediction of potential and viscous flow in axisymmetric propulsion system inlets has been briefly described. The method has already proven to be a very useful and powerful tool for both analysis and design purposes. The various elements of the method are constantly being updated, thus improving both its versatility and accuracy. It is probably the best tool available at present for analyzing the compressible viscous flow in axisymmetric inlets at arbitrary angle of attack and will continue to be until exact three-dimensional compressible inlet flow computer programs become practical.

### REFERENCES

1. Stockman, N. O.; and Lieblein, S.: Theoretical Analysis of Flow in VTOL Lift Fan Inlets Without Crossflow. NASA TN D-5065, 1969.
2. Lieblein, S.; Yuska, J. A.; and Diedrich, J. H.: Performance Characteristics of a Model VTOL Lift Fan in Crossflow. Journal of Aircraft, Vol. 10, No. 3, March 1973, pp. 131-136.
3. Stockman, N. O.; Loeffler, I. J.; and Lieblein, S.: Effect of Rotor Design Tip Speed on Aerodynamic Performance of a Model VTOL Lift Fan Under Static and Crossflow Conditions. Journal of Engineering for Power, Trans. ASME, Series A, Vol. 95, No. 4, Oct. 1973, pp. 293-300.
4. Stockman, N. O.: Potential Flow Solutions for Inlets of VTOL Lift Fans and Engines. Analytical Methods in Aircraft Aerodynamics, NASA SP-228, Washington, D.C., 1970, pp. 659-681.
5. Albers, J. A.; and Gregg, J. L.: A Computer Program to Calculate Laminar, Transitional, and Turbulent Boundary Layers for Compressible Axisymmetric Flow. NASA TN D-7521, 1974.
6. Albers, J. A.; and Stockman, N. O.: Calculation Procedures for Potential and Viscous Flow Solutions for Engine Inlets. Journal of Engineering for Power, Trans. ASME, Series A, Vol. 97, No. 1, January 1975, pp. 1-10.

7. Albers, J. A.; Stockman, N. O.; and Hirn, John J.: Aerodynamic Analysis of Several High Throat Mach Number Inlets for the Quiet Clean Short-Haul Experimental Engine. NASA TM X-3183, Jan. 1975.
8. Felderman, E. John; and Albers, J. A.: Comparison of Experimental and Theoretical Boundary-Layer Separation for Inlets at Incidence Angle at Low-Speed Conditions. NASA TM X-3194, February 1975.
9. Hess, J. L.; and Smith, A. M. O.: Calculation of Potential Flow About Arbitrary Bodies. Progress in Aeronautical Sciences, Vol. 8, O. Kuchemann, ed., Pergamon Press, 1967, pp. 1-138.
10. Stockman, N. O.; and Button, S. L.: Computer Programs for Calculating Potential Flow in Propulsion System Inlets. NASA TM X-68278, 1973.
11. Lieblein, S.; and Stockman, N. O.: Compressibility Correction for Internal Flow Solutions, Journal of Aircraft, Vol. 9, No. 4, April 1972, pp. 312-313.
12. Hess, J. L.; and Martin, R. P.: Improved Solution for Potential Flow About Arbitrary Axisymmetric Bodies by the Use of a Higher-Order-Surface Source Method. NASA CR-134694, July 1974.

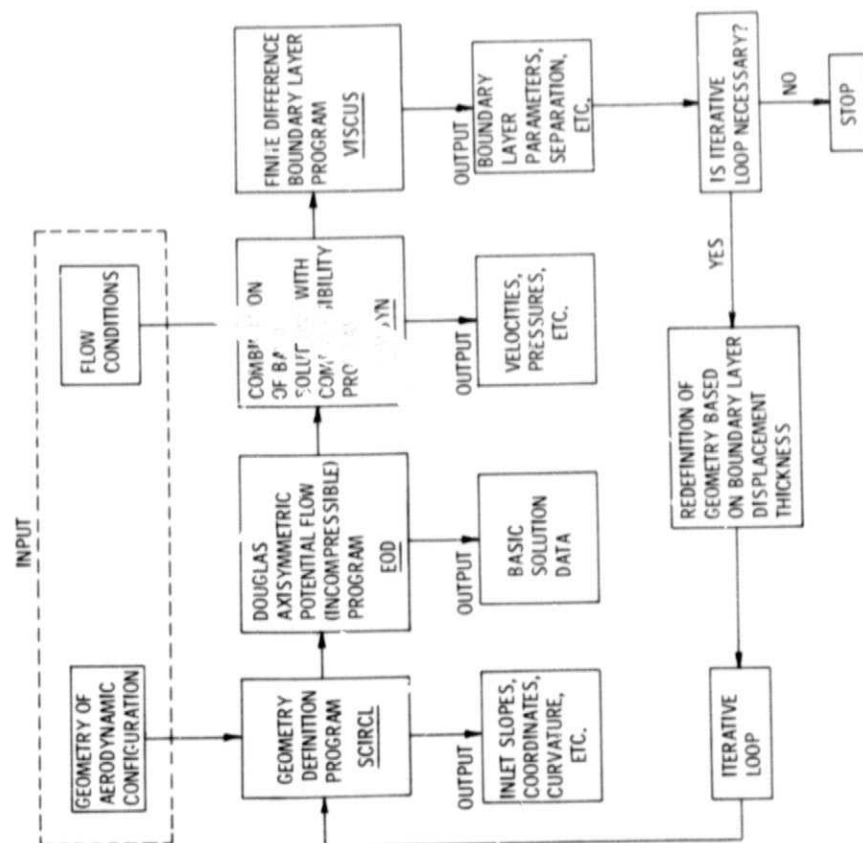


Figure 1 - Schematic of inlet programs.

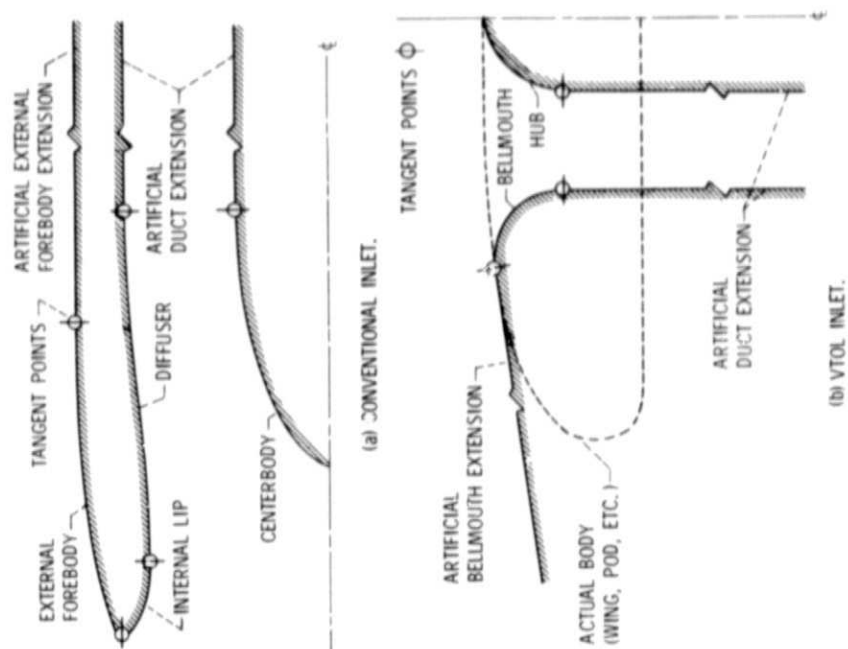


Figure 2 - Representative inlet geometries for potential flow solutions.

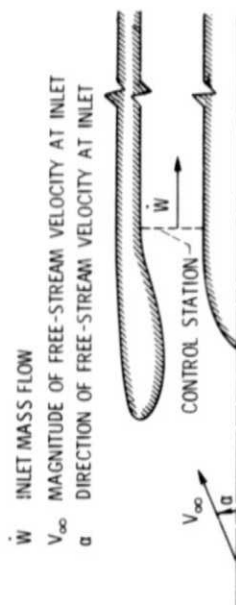


Figure 3 - Flow conditions for combined solution.

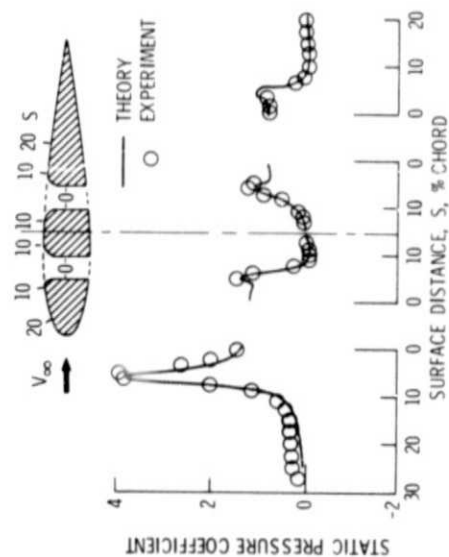


Figure 4 - Comparison with experiment of fan-in-wing surface pressure distribution. Average rotor inlet Mach number,  $\bar{M}_c = 0.19$ ,  $M_\infty = 0.05$ .

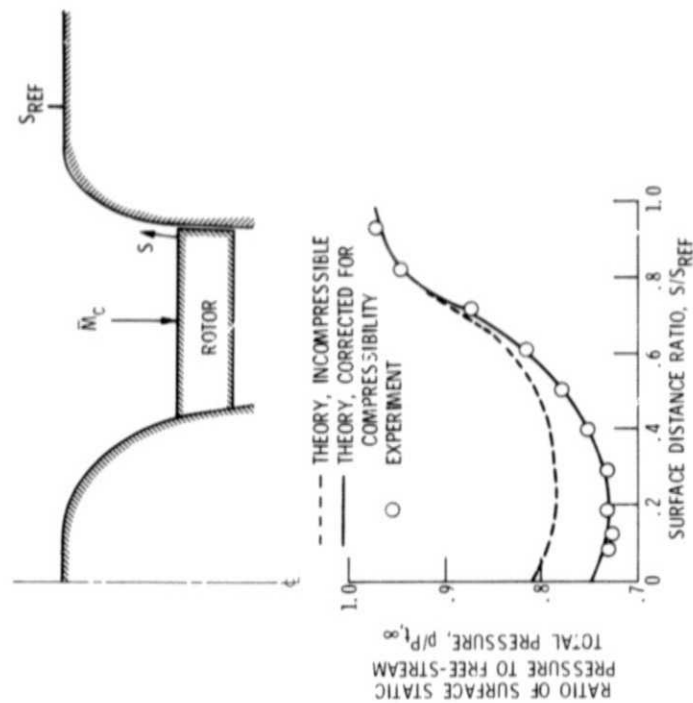
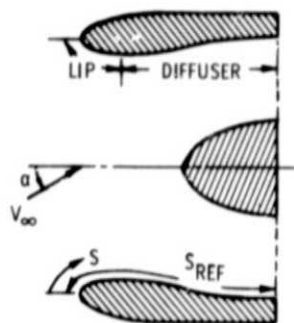
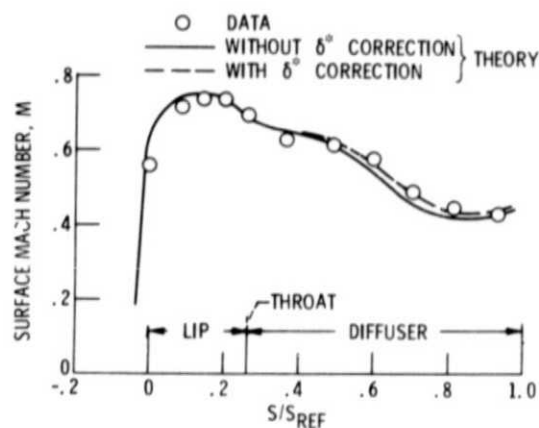


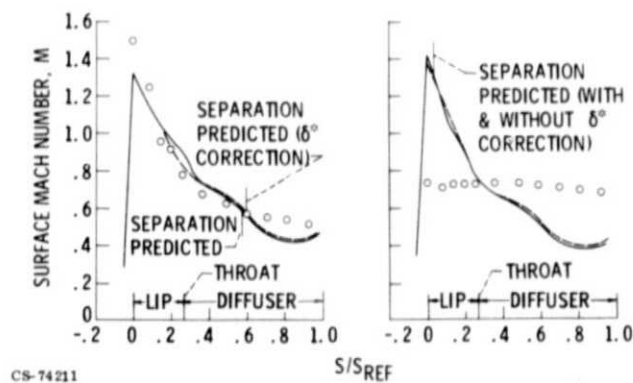
Figure 5 - Comparison with experiment of fan-in-pod inlet surface pressure distribution. Static condition,  $V_\infty = 0$ . Average rotor inlet Mach number,  $\bar{M}_c = 0.57$ .



(a) GEOMETRY.



CS-74214

(b) BOUNDARY LAYER ATTACHED,  $\alpha = 0$ .Figure 6. - Sonic inlet with boundary layer,  
 $M_{th} = 0.50$ ,  $M_{\infty} = 0.13$ .

CS-74211

(c) DIFFUSER SEPARATION,  
 $\alpha = 40^\circ$ .(d) LIP SEPARATION,  
 $\alpha = 50^\circ$ .

Figure 6. - Concluded.



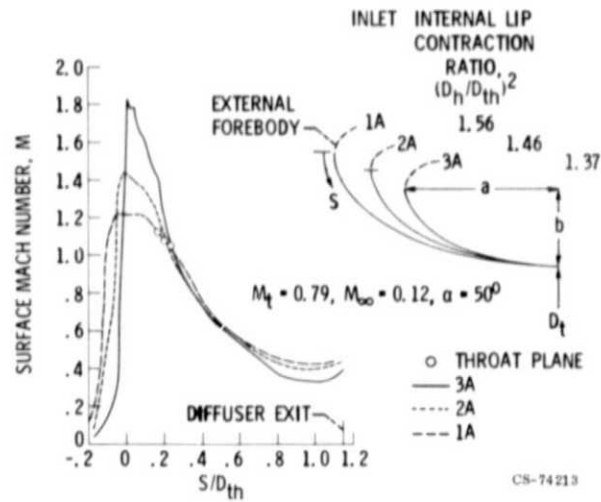


Figure 7. - Effect of internal lip contraction ratio on surface Mach number distribution.

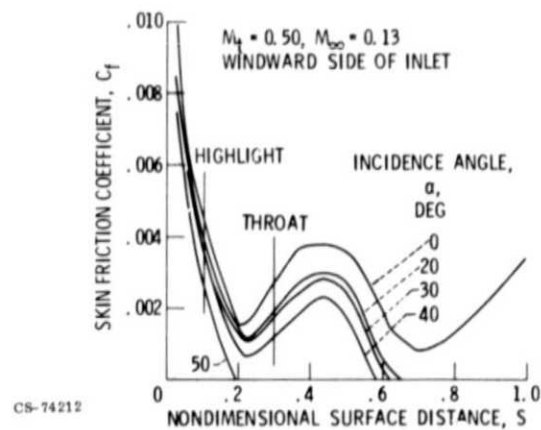


Figure 8. - Theoretical skin friction coefficients (without  $\delta^\circ$  correction for centerbody retracted).

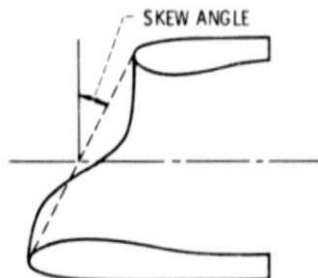


Figure 9. - Scoop inlet.